Electronic structure of periodically δ-doped GaAs:Si

L. Chico, F. García-Moliner, and V. R. Velasco
Instituto de Ciencia de Materiales, Consejo Superior de Investigaciones Científicas, Serrano 123, 28006 Madrid, Spain
(Received 29 December 1992; revised manuscript received 5 May 1993)

The electronic structure of periodically doped GaAs:Si systems has been self-consistently calculated with a Hedin-Lundqvist local-density functional for exchange and correlation. The influence of the periodic spacing d, the areal impurity concentration N_d, and the spread of the impurity distribution have been investigated. Miniband widths and gaps, potential-well depths, and Fermi-level position have been studied between $d = 100$ and 500 Å, thus following the transition from superlattice behavior to independent well regime. The results are used to interpret some observed photoluminescence spectra.

I. INTRODUCTION

As improvements in epitaxial growth have allowed for a better control of impurity doping in semiconductors there has been increasing interest in the δ-doped systems, thus called because of the ultimate target of achieving a strict localization of the impurities in one atomic layer.[1,2] Raman spectroscopy,[3,4] infrared absorption,[5] magnetotransport,[6] and photoluminescence[3–5,7] have been used in experimental studies of these systems.

A new type of superlattice is produced in which there is only one bulk material but the potential is modulated by periodic δ doping. If only one type of dopant is used, e.g., donors, then in the uncompensated sample the extrinsic electrons screen the ionized donors and produce inhomogeneous potentials about the plane of the donor sheets which are to be obtained self-consistently. Some self-consistent calculations have been recently reported.[7–9] The purpose of this paper is to describe some further calculations which complement the results obtained in these studies[7–9] in a significant way and they also allow for the interpretation of some photoluminescence experiments,[3] giving strong support to the claims presented there.

II. MODEL AND CALCULATION

We first study periodical δ doping of Si in GaAs with a donor impurity distribution of the form

$$n(z) = N_d \sum_{n=-\infty}^{+\infty} \delta(z - nd) \tag{1}$$

and then investigate the effect of a smearing out the impurity density in the form of Gaussian distributions:

$$n(z) = \frac{N_d}{\sqrt{2\pi\sigma^2}} \sum_{n=-\infty}^{+\infty} e^{-(z-nd)^2/2\sigma^2}, \quad \sigma = \frac{\Delta z}{2\sqrt{2\ln 2}}. \tag{2}$$

The half-width Δz was chosen to be between 20 and 40 Å, which appear to be realistic figures for current experimental devices[10,11] once the effect of the substrate temperature T_s on the segregation of Si has been clarified. High values of T_s, of order 600 °C (Ref. 10) seem to be convenient to ensure the growth of good quality, fairly defect-free structures. However with such temperatures Si tends to diffuse considerably, with a spreading of the doped zone which can reach values of order 100 Å,[10,11] so a compromise must be sought between the quality of the structure and the control of the impurity segregation. It is found[10] that for $T_s < 530$ °C there is a significant reduction in Si diffusion and values of Δz of the order quoted above can be achieved, so we shall take these values as realistically representative in order to assess the effects of impurity spreading.

For areal impurity densities below 10^{11} cm^{-2} it would be quite unrealistic to assume a continuous positive charge distribution of the ionized impurities, but this can be assumed beyond 1.3×10^{11} cm^{-2}.[12] On the other hand, beyond 8×10^{12} cm^{-2} a saturation of the electronic density is observed,[1,6,11] that is, Hall effect measurements yield an areal electron concentration of 8×10^{12} cm^{-2} which stays constant even when the nominal impurity doping is increased. In this study we shall consider areal impurity concentrations between 1 and 7×10^{12} cm^{-2}, which correspond to the experimental data we shall later discuss. In this range we can assume that all the donors are ionized and that their areal density is continuous. The values of the superlattice period d here studied vary between 100 and 500 Å, which cover the range from a superlattice to a system of effectively independent quantum wells.

We use a one-band effective-mass model and calculate self-consistently the electronic states and the one-electron potential $V(z)$ as the sum of the Hartree-Poisson potential and an exchange and correlation potential which we approximate by the Hedin-Lundqvist local-density functional.[13] Other parametrizations of the exchange and correlation density functional are possible and yield rather similar results for the one-electron density of states from which the electronic charge density $\rho(z)$ is self-consistently calculated. We have used the same scheme employed in a recent study of modulation doped quantum wells, which appears to work well,[14] although any use of a local-density functional is to be taken of course as just an approximation.

For the integration of the Schrödinger equation we use the full transfer matrix discussed in Ref. 15, which transfers both amplitude and derivative, the amplitude being in this case the envelope function $F_{jq}(z)$ for the subband j with one-dimensional (1D) momentum q associated to

the period d of the superlattice. By definition

$$M(z,z_0)\begin{pmatrix} F(z_0) \\ F'(z_0) \end{pmatrix} = \begin{pmatrix} F(z) \\ F'(z) \end{pmatrix}, \tag{3}$$

where $M(z,z_0)$ is the 2×2 full transfer matrix which transfers from a chosen reference point z_0 to a variable end point z. The relationship between M and the Green function, from which the local density of states and the electron charge density can be calculated, is fully discussed in Refs. 16 and 17. Furthermore, for the system with period d:

$$M(z_0+d,z_0)\begin{pmatrix} F(z_0) \\ F'(z_0) \end{pmatrix} = \begin{pmatrix} m_{AA} & m_{AD} \\ m_{DA} & m_{DD} \end{pmatrix}\begin{pmatrix} F(z_0) \\ F'(z_0) \end{pmatrix} = e^{iqd}\begin{pmatrix} F(z_0) \\ F'(z_0) \end{pmatrix}, \tag{4}$$

where m is the full transfer matrix across one entire period, which leads to the well-known eigenvalue equation

$$\cos qd = \tfrac{1}{2}\mathrm{tr}\, m \tag{5}$$

in terms of the energy-dependent full transfer matrix.

The Bloch-Floquet property (4) allows us to obtain the derivative at some chosen point z_0 by means of the algebraic relationship

$$F'(z_0) = \frac{(e^{iqd} - m_{AA})}{m_{AD}} F(z_0) \tag{6}$$

whence we can obtain the wave-function amplitudes from the first row of (3) and then use a standard normalization scheme. Alternatively, we can obtain the Green function for which there is no need to normalize.[17] The calculation also yields self-consistently the position of the Fermi level E_F, from the condition that the total number of electrons must equal the total number of donors. In practical terms we have stopped the calculation when the mean square deviation of the total one-electron potential in two consecutive cycles is ≤ 0.1 meV.

The scheme just outlined allows us to treat on the same footing long and short periods without resorting to a separate treatment for wide minibands, typical of short periods.[7] The numerical labor involved is also insensitive to changes in d, which is a substantial practical advantage over schemes based on a plane-wave representation, where long periods require a substantial increase in the number of components in order to achieve an adequate description of the electronic wave functions.[8]

III. RESULTS AND COMMENTS

We have studied superlattices with d=100, 300, and 500 Å with values of $N_d = n_d \times 10^{12}$ cm^{-2} with n_d=1,3,5,7, as well as some specific cases for which experimental information is available. Besides strict δ doping we have also studied Gaussian distributions with Δz equal to 20 and 40 Å. The parameters used for GaAs are m^*=0.0665m_0 and ε=12.5 in Gaussian units.

Figure 1 displays the results for a superlattice with $n_d = 5$, $d = 300$ Å, and $\Delta z = 20$ Å, and will serve us to show the notation. The shaded areas are the allowed energies for $\kappa = 0$ when q varies over the 1D Brillouin zone, i.e., the superlattice minibands. The dashed line is the Fermi level of the system, and V_0 is the maximum potential height.

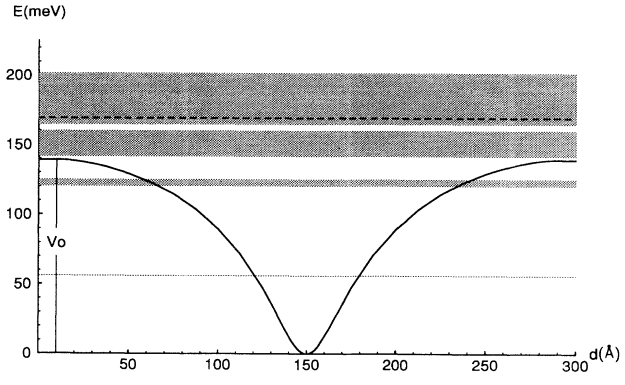

FIG. 1. Self-consistent one-electron potential profile for a system with periodic doping with an impurity spreading Δz = 20 Å, impurity density $n_d = 5$, and superlattice period d= 300 Å. The shaded zones are the miniband energies, i.e., the allowed energies for $\kappa = 0$. The dashed line is the Fermi level and V_0 denotes the maximum depth of the wells. All energies are referred to the bottom of the potential well.

We have calculated $V(z)$, $\rho(z)$, miniband edges, and Fermi-level position studying the effects of changing the key parameters N_d and d. The general aspect of the potential and charge density profiles does not change in any significant manner. It is more interesting to look at the changes in V_0, E_F, and miniband edges, shown in Fig. 2 as a function of d (varying between 100 and 500 Å) for different values of N_d, always in the range of 10^{12} cm^{-2}, as indicated. These results contain the information which is physically significant in practice. Obviously V_0 increases with increasing N_d, and also, for fixed N_d, as d increases. When the wells are wide apart and their potentials have negligible overlap, the system behaves as a set of independent isolated wells, while as d decreases their coupling increases and the system tends to show superlattice behavior. One of the purposes of this study is precisely to ascertain when this takes place, as this is a practical issue in the analysis of the experimental data to be discussed below.

Generally speaking our results can be described as follows.

(i) For d=100 Å all cases show definite superlattice behavior. For the high impurity densities all minibands still show a width which should be experimentally detectable: The lowest one, which is always the narrowest, reaches values of order 30 meV at least. The total number of occupied minibands is never larger than two.

(ii) For d=500 Å all cases show separate well behavior. The occupied miniband widths are negligible for all values of N_d and E_F and V_0 tend to be very close. There are between three and four occupied minibands.

(iii) For intermediate values of $d \approx 250$ Å the lowest miniband—always occupied—is very narrow, so in this energy range the wells are effectively independent on this account. However, the next one is significantly wide. Population of this miniband starts for $N_d \geq 3 \times 10^{12}$ cm^{-2} when its width is at least ≈20 meV, so in this energy range superlattice behavior sets in.

The effect of spreading out the impurity concentration is to change considerably the $V(z)$ and $\rho(z)$ profiles and the position of the minibands relative to the bottom of the wells (Fig. 3), in agreement with the conclusions reached in Ref. 9. However, this need not mean that the electronic properties of the system change appreciably. We have studied the subband populations and find these to be very little affected, also in agreement with Ref. 9. Furthermore, and more significantly, we have studied the values of the gaps and miniband widths, as well as their relative positions, which are the magnitudes more directly related to experimental results, and find these to be rather insensitive to plausible changes in the impurity distribution.

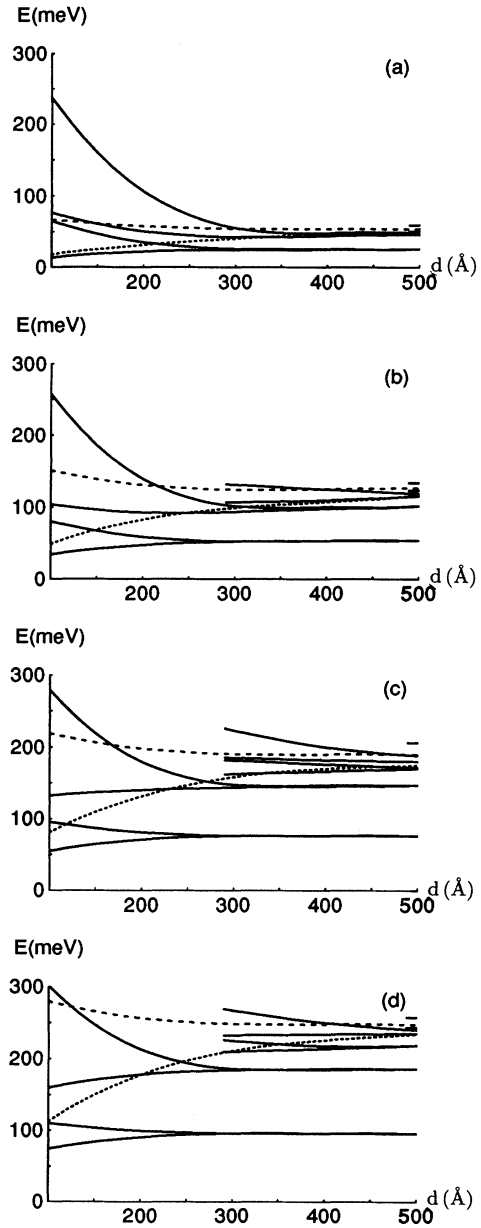

FIG. 2. Full lines: miniband edges ($\kappa = 0$, q spanning the 1D Brillouin zone). Dotted line: values of the well depth V_0 (see Fig. 1). Dashed line: E_F. All energies are referred to the bottom of the potential wells and periodic δ doping is assumed. Values of n_d are as follows: (a) 1; (b) 3; (c) 5; (d) 7.

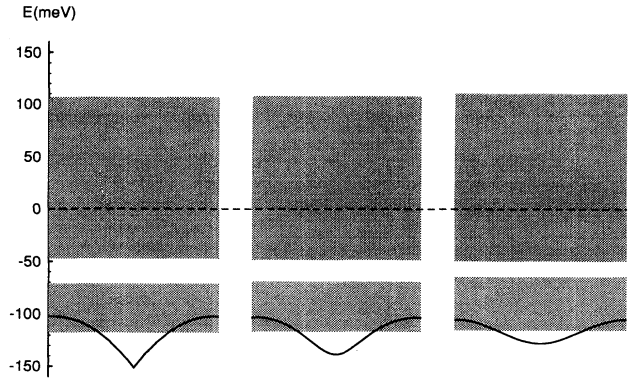

FIG. 3. Potential profiles, miniband energies ($\kappa = 0$, shaded), and Fermi level (dashed line) for superlattices with $n_d = 3$, $d = 100$ Å and impurity spreadings of 0, 20, and 40 Å, from left to right. All energies are referred to the Fermi level.

Photoluminescence spectroscopy appears to provide a suitable experimental tool for the investigation of these superlattices. The technique is rather unsuitable for isolated wells because the potential which is attractive for the electrons is repulsive for the photocreated holes, which reduces considerably the overlap between the electron and hole wave functions. This difficulty is circumvented in the superlattice due to the periodic modulation of the potential, whence an enhancement of the recombination rate. Quite recently these systems were studied by means of photoluminescence techniques and it was pointed out that the difference between the 3D Fermi energy E_F^{3D} and the observed width of the main photoluminescence peak W_{PL} provides strong evidence that electrons are confined in the space charge potential and that subbands broaden into minibands as the layer separation is reduced. We have studied three of the samples experimentally studied by photoluminescence[3] and some parameters and results are summarized in Table I. The presence of defects in the samples may relax the momentum conservation selection rule for optical transitions, so that for free electron behavior one might expect the equivalent 3D Fermi energy E_F^{3D} to give a fair account of W_{PL}. Firstly a comparison of columns three and four

TABLE I. d, superlattice period. N_d, areal impurity density. E_F^{3D}, 3D Fermi energy estimated from the equivalent uniform carrier density. E_F, Fermi energy calculated self-consistently. W_{PL}, experimental width of the dominant PL peak (Ref. 3). Δ_p, width of the highest miniband with significant population in the self-consistent calculation.

d (Å)	N_d (10^{12} cm^{-2})	E_F^{3D} (meV)	E_F (meV)	W_{PL} (meV)	Δ_p (meV)
100	1.4	68	69	43	51
200	1.2	39	57	25	32
500	1.0	18	33	7	3

shows a significant disagreement between E_F^{3D} and the actual self-consistent result E_F for large d, and very good agreement for d=100 Å. From the results shown in Fig. 2 we would expect that most of the free electron population is in energy levels above V_0 and is therefore largely unlocalized. However, although this might account for the numerical agreement between E_F^{3D} and E_F, the real behavior is not actually free-electron-like. Moreover, as already noted in Ref. 3, E_F^{3D} disagrees with the observed values of W_{PL} (column five). In fact the assumption that one can identify the observed width of the photoluminescent peak with the Fermi energy is strongly dependent upon the assumption of free electron behavior and it is clear that this is not the case even for d=100 Å.

The results of our calculations are in line with the interpretation put forward in Ref. 3. Thus it seems more plausible to try and interpret peak widths as giving an approximate measure of the widths of the occupied minibands. Since different peaks are sometimes observed we should associate the distances between peaks with some approximate mean distance between minibands.

This expectation is fairly borne out by the comparison between columns five and six. It is seen that W_{PL} agrees indeed substantially better with Δ_p than it does with E_F. For the sample with d=200 Å according to our self-consistent calculations there should be two occupied minibands but the population of the second one is negligible compared with that of the first one, which is the one for which we calculate Δ_p. For the sample with d=500 Å the value given in the fifth column of the table corresponds to the dominant peak. Another two peaks have also been observed, which we can associate with another two populated subbands which, according to our calculation, should have some significant population. Due to poor spectral resolution it is extremely difficult to obtain any reliable estimate of their widths, but the distances between the peaks can be estimated as 20 and 15 meV, in fair agreement with our estimated mean distances between occupied minibands of 20 and 8 meV, respectively.

Another photoluminescence spectrum has been reported[7] for a superlattice with d=300 Å and n_d=5, which can be likewise interpreted. In our calculation we find that there should be four occupied minibands, the two lowest ones being substantially narrower. Two peaks can be clearly identified in the experimental spectrum, which we can associate with the third and fourth minibands, and also some structure is observed at lower energies which one could interpret as indicative of two peaks at 1.430 and 1.495 eV. On this basis the three distances between the four peaks are 65, 15, and 15 meV. Our estimate for the mean distances between the corresponding minibands yields 70, 25, and 10 meV, which is again as fair as one could expect.

The quantitative agreement with experimental data is only approximate, as corresponds to the avowed approximations made in the proposed interpretation. The measure of the "mean distance" between bands, for instance, is rather vague. But the whole interpretation seems quite plausible and in that sense everything fits within a picture which does unmistakeably bear out the quasi-2D nature of the spectrum, even for d=100 Å, when most of the electron population is above the top of the potential wells. These electrons are highly delocalized but there is no way to identify W_{PL} with the Fermi energy, even if this is self-consistently calculated, since a gap exists between occupied delocalized states which do not therefore have free-electron-like behavior.

While allowing us to see the influence of the key parameters, N_d and d, this also provides a reasonable basis to attempt an actual calculation of the photoluminescence spectrum.

ACKNOWLEDGMENTS

This work was carried with partial support of the Spanish CICYT (Grant No. MAT91-0738) and the Research Scholarships Programme of the Spanish Ministry of Education and Science (L.Ch.). We wish to express our warmest gratitude to Professor R. Pérez-Alvarez for his generous help with innumerable discussions which provided a great deal of help and stimulation.

[1] E. F. Schubert, A. Fischer, and K. Ploog, IEEE Trans. Electron Devices **ED-33**, 625 (1986).
[2] K. Ploog, J. Cryst. Growth **81**, 304 (1987).
[3] A. C. Maciel, M. Tatham, J. F. Ryan, J. M. Worlock, R. E. Nahory, J. P. Harbison, and L. T. Florez, Surf. Sci. **228**, 251 (1990).
[4] J. Wagner, A. Fischer, and K. Ploog, Phys. Rev. B **42**, 7280 (1990).
[5] E. F. Schubert, Surf. Sci. **228**, 240 (1990).
[6] A. Zrenner, F. Koch, and K. Ploog, Surf. Sci. **196**, 671 (1988).
[7] M.-L. Ke, J. S. Rimmer, B. Hamilton, M. Missous, B. Khamsehpour, J. H. Evans, K. E. Singer, and P. Zalm, Surf. Sci. **267**, 65 (1992).
[8] F. A. Reboredo and C. R. Proetto, Solid State Commun. **81**, 163 (1992).
[9] M. H. Degani, J. Appl. Phys. **70**, 4362 (1991).
[10] M. Santos, T. Sajoto, A.-M. Lanzillotto, A. Zrenner, and M. Shayegan, Surf. Sci. **228**, 255 (1990).
[11] H. C. Nutt, R. S. Smith, M. Towers, P. K. Rees, and D. J. James, J. Appl. Phys. **70**, 821 (1991).
[12] E. I. Levin, M. E. Raikh, and B. I. Shklovskii, Phys. Rev. B **44**, 11 281 (1991).
[13] L. Hedin and B. I. Lundqvist, J. Phys. C **4**, 2064 (1971).
[14] L. Chico, W. Jaskólski, and F. García-Moliner, Phys. Scr. **47**, 284 (1993).
[15] M. E. Mora, R. Pérez, and Ch. B. Sommers, J. Phys. **46**, 1021 (1985).
[16] F. García-Moliner, R. Pérez-Alvarez, H. Rodríguez-Coppola, and V. R. Velasco, J. Phys. A **23**, 1405 (1989).
[17] F. García-Moliner and V. R. Velasco, *Theory of Single and Multiple Interfaces* (World Scientific, Singapore, 1992).